

# RATES OF LIGHT GAS PRODUCTION BY DEVOLATILIZATION OF COALS AND LIGNITE

R. F. Weimer and D. Y. Ngan

Air Products and Chemicals, Inc.; Allentown, Pennsylvania, 18105

## INTRODUCTION

The kinetics of coal pyrolysis are important in many coal conversion processes which operate under conditions of relatively moderate temperatures (400° to 1000°C). Such processes range from in situ coal gasification (1) to flash hydropyrolysis (3), having anticipated coal residence times in the region of pyrolysis temperatures of between  $10^{-1}$  and  $10^4$  seconds - a range of five orders of magnitude.

Although many models have been postulated for coal devolatilization (4), Howard and his co-workers (2,4) have shown that the use of a statistical distribution of activation energies can provide "valuable insight into the overall or global kinetics of the [pyrolysis] process," particularly with regard to explaining the effects of heating rate. They therefore state (4) that, "For a designer seeking a correlation of devolatilization yields, [the distributed activation energy model] combined with a description of secondary reactions is presently the best recommendation." Ciuryla et al. (6) have since shown that the parameters (mean activation energy, standard deviation of the energy distribution, and total potential volatilization) obtained by fitting total weight loss data obtained at heating rates of 40 and 160°C/min, for a Montana lignite and a Pittsburgh Seam bituminous coal, are close to the values reported by Anthony and Howard for the same coals at heating rates of 100 to 10,000°C/sec.

The distributed activation energy model has not previously been applied to data for the yields of individual molecular species from coal pyrolysis. It has normally been assumed (with good results for data obtained over a narrow range of heating rates) that the yields of individual species can be modelled by a small set of individual reactions representing the major mechanisms for their production. However, it has been recognized (2) that the parameters obtained from such models are only "effective" values which may have no fundamental significance. It can be shown (see below) that the values typically obtained from models having a small number of individual reactions cannot be applied over a wide range of heating rates.

## EXPERIMENTAL

### Coal Samples

The North Dakota lignite and Illinois No. 6 bituminous coal samples used in this study were provided by the Pennsylvania State University. The Pittsburgh Seam bituminous and Wyodak subbituminous coal samples were obtained from Commercial Testing and Engineering Company; these samples were ground under inert atmosphere. Proximate and ultimate analyses of the coals studied are given in Table 1. Sized, 40 x 80 mesh, samples were used in all runs.

### Apparatus

The primary apparatus used in obtaining the results reported herein was a 6-gram-capacity thermobalance built specifically for Air Products' laboratories by Spectrum Products, Inc. This apparatus is essentially identical to equipment which was previously in existence at Case-Western Reserve University (5). The apparatus consists of a cylindrical basket, containing the coal sample, which is suspended from a balance arm into an externally heated Haynes 25 superalloy tube. Although the apparatus is capable of operation at pressures up to 1500 psi, only results obtained at atmospheric pressure, in helium, are reported here. Heating rates were monitored by thermocouples

on the tube wall, and also inside the tube near the basket, it having been determined (by placing a thermocouple in the basket itself) that the differences between the sample temperature and the wall temperature were small.

### Experimental Procedure

Approximately 3 gms of dry, 40 x 80 mesh, coal were placed inside the sample basket and lowered into the reactor at room temperature. After purging the system with helium, the reactor was heated. The temperature, monitored by a thermocouple located immediately below the sample basket, the helium flow rate, and the sample weight were continuously recorded. Gas samples were periodically collected by syringes through a septum in the heated exit line. These samples were subsequently analyzed using a Perkin-Elmer Sigma-1 gas chromatograph.

The helium flow rate was maintained at approximately 700 cc/min. Due to the heat capacity of the tube and furnace, and to heat losses from the furnace, the heating rate was not constant during the experiments; however, the observed rates can be approximated by the formula

$$\frac{dT}{dt} = 10.8 - 0.00642 \cdot T$$

where  $T$  = sample temperature,  $^{\circ}\text{C}$ , and  $t$  = time, minutes. The actual recorded time/temperature data were used in the computer analysis of the results.

### Kinetic Model

Coal pyrolysis has frequently been assumed to be described by a set of parallel first-order reactions (1,2,4). For each reaction,  $i$ , the corresponding devolatilization rate is

$$\frac{dV_i}{dt} = k_i e^{-\frac{E_i}{RT}} (V_i^* - V_i) \quad 1)$$

where  $k_i$  is the preexponential factor and  $E_i$  is the activation energy of reaction  $i$ ;  $V_i$  is the amount of volatile product produced by reaction  $i$  up to time  $t$ ;  $V_i^*$  is the amount of product which could potentially be produced;  $T$  is the absolute temperature, and  $R$  is the gas constant. The total yield from reaction  $i$  at time  $t$  is therefore

$$\frac{V_i^* - V_i}{V_i^*} = \exp \left\{ -k_i \int_0^t e^{-\frac{E_i}{RT}} dt \right\} \quad 2)$$

For the case of constant heating rate,  $m = dT/dt$ , it has been shown (2) that, since  $E_i/RT \gg 1$  for coal pyrolysis reactions, the solution of Equation 2 is

$$\frac{V_i^* - V_i}{V_i^*} = \exp \left\{ -\frac{k_i RT^2}{mE_i} e^{-\frac{E_i}{RT}} \right\} \quad 3)$$

(This equation may be extended to include a holding period at pyrolysis temperature and/or the subsequent cool-down period, as shown in the Appendix.)

Integration of Equation 2 for the case of nonconstant heating rate may easily be done numerically; however, provided that

$$\frac{RT}{E_i} \cdot \frac{T}{m} \cdot \frac{dm}{dT} \ll 1$$

Equation 3 with  $m = m(T)$  can be used.

The distributed activation energy model assumes that the activation energy for producing volatile material (or a specific volatile product) is normally distributed about a mean value,  $E_{i0}$ , with  $k_i$  constant. The result, analogous to Equation 3, is

$$\frac{V_i^* - V_i}{V_i^*} = \frac{1}{\sigma\sqrt{2\pi}} \int_0^{\infty} \exp \left[ -\frac{k_i RT^2}{mE} e^{-\frac{E}{RT}} \right] \exp \left[ -\frac{(E-E_{i0})^2}{2\sigma^2} \right] dE \quad 4)$$

where  $\sigma$  is the standard deviation of the energy distribution. (In practice, integration from  $E = 1$  kcal/mol to  $E = E_{i0} + 4\sigma$  is adequate for analyzing the data.)

The rate of devolatilization at temperature  $T$  is

$$\frac{1}{V_i^*} \frac{dV_i}{dt} = \frac{k_i}{\sigma\sqrt{2\pi}} \int_0^{\infty} e^{-\frac{E}{RT}} \exp \left[ -\frac{k_i RT^2}{mE} e^{-\frac{E}{RT}} \right] \exp \left[ -\frac{(E-E_{i0})^2}{2\sigma^2} \right] dE \quad 5)$$

#### RESULTS AND DISCUSSION

Figures 1 through 5 present the pyrolysis rate data, for each of the five coals, for the four major noncondensable products of pyrolysis (hydrogen, carbon monoxide, carbon dioxide, and methane). The total weight loss is also shown. The initial appearance of these species occurs in the same order for all of the coals:  $CO_2$  appears first, followed by  $CO$ ,  $CH_4$ , and, finally,  $H_2$ . However, the maximum rate of  $CO$  production does not occur until well after that of methane; the temperature of the maximum rate of  $CO$  production is nearly coincident with that of the maximum rate of hydrogen production (about  $700^\circ C$ ). (The  $CO$  production rate is actually bimodal, with a small peak at about  $450^\circ C$  and a larger peak at about  $700^\circ C$ , for the low-rank coals.) The observed peaks for  $C_2$  and  $C_3$  hydrocarbons (not shown) occur at the same temperature as those for methane. The major differences among the coals are in the amounts of  $CO$  and  $CO_2$  produced, which are, of course, related to the vastly differing oxygen contents of the feed coals.

These results are similar to data reported by Campbell (1) for the slow ( $3.3^\circ C/min$ ) pyrolysis of 50-gram samples of 6 x 12 mesh Wyodak coal, although his total yields of light hydrocarbons were greater than those reported here.

The values found by fitting the Gaussian distributed activation energy model to the data are listed on Table 2. Except for the  $CO$  data, which are clearly bimodal, the single Gaussian distribution provides a reasonable first approximation of the data. Except for the Pittsburgh Seam bituminous coal (which yielded very little  $CO$  and  $CO_2$ ), the mean activation energies increase in the order  $CO_2$ ,  $CO$  (first peak),  $CH_4$ ,  $CO$  (second peak), and  $H_2$ . The surprising result is the close correspondence of the values obtained for both  $E_{i0}$  and  $\sigma$  for each component from coals of widely differing rank. This suggests that the major mechanisms for the production of these materials are the same for all of the coals.

Table 3 lists, for comparative purposes, the parameters obtained by Campbell by fitting his data to one to three first-order reactions per compound. Since  $\sigma$  is zero in this model, it is necessary to allow  $k_j$  for each reaction to vary. The result is a set of extremely low values for both  $k_j$  and  $E_j$  for all of the reactions. For example, Campbell's value of  $E_j$  for hydrogen production is 19.5 kcal/g mole, compared to the  $E_0$ 's of 73 to 75 kcal/mol in Table 2, and a typical value (1) of 88 kcal/mol for C-H bond breakage. The small absolute values of  $k_j$  and  $E_j$  in Campbell's model result from fitting a yield distribution which is spread broadly over temperature with a small number of reactions.

The effect of temperature on flash pyrolysis yields has been studied by Suuberg *et al.* (2) for a Montana lignite. Suuberg's results (Figures 6 and 7), which are total yield data for heating small (15 mg) samples at 1000°C/sec to the indicated peak temperature, and then cooling immediately at a rate of 200°C/sec, show the same trends in the order of the appearance of the various species as do the slow pyrolysis data; in addition, Suuberg's ultimate yields of each of the light gases are similar to those observed upon slow pyrolysis of lignite and subbituminous coal in our experiments.

Suuberg also fit his results using a small number of first-order reactions to describe the yields of each species; his parameters are shown in Table 4. Reasonable values of  $E_0$  were obtained, but the predicted yield curves, as shown on Figures 6 and 7, are notably stepwise in appearance. Also plotted on Figures 6 and 7 are the curves obtained by using the lignite pyrolysis parameters of Table 2, and the distributed activation energy model, to predict the flash pyrolysis yields. The predictions fit the data almost as well as Suuberg's own model, provided only that  $V_j^*$  for each species is allowed to vary. This illustrates the ability of the distributed activation energy model to fit both slow and fast pyrolysis data with the same values for the activation energy parameters. In contrast, the slow pyrolysis parameters reported by Campbell would predict almost no reaction under Suuberg's conditions, since his values of  $k_j$  are too small to permit any significant reaction in a time of the order of one second.

Finally, the problem inherent in applying Suuberg's model and parameters to slow pyrolysis rate data is illustrated - for the case of CO<sub>2</sub> formation from lignite - by Figure 8. The use of a small number of individual equations requires that the products appear in a few sharply defined peaks (corresponding to the steep steps in the yield curves) in contrast to the broadly distributed slow pyrolysis data.

#### CONCLUSIONS

A first-order model with distributed activation energies has the potential for explaining the effect of heating rate on the primary production of light gases (H<sub>2</sub>, CO, CO<sub>2</sub>, CH<sub>4</sub>) during the devolatilization of coal; models based on small sets of first-order reactions with nondistributed activation energies do not have this potential. The activation energy distributions for the production of these species obtained from atmospheric-pressure pyrolysis, under inert atmosphere, are remarkably insensitive to coal rank. Data on identical samples of coal, over a wide range of heating rates, would be needed to confirm the validity of this approach to understanding pyrolysis kinetics.

#### ACKNOWLEDGEMENTS

Dr. K. J. Anselmo of the Management Information Department of Air Products and Chemicals, Inc., is acknowledged for his assistance in developing the computer curve-fits of the data. Mr. S. A. Motika of the Corporate Research and Development Department of Air Products and Chemicals, Inc., is acknowledged for his work in the preparation of coal samples and the operation of the apparatus used in this research.

## APPENDIX

### Extension of Model Beyond Heating Period

The time-temperature history of much of the published data on coal pyrolysis may be divided into three regions:

1. Heat-up at a constant rate,  $m_1$ , to a peak temperature,  $T_1$ .
2. Holding at temperature,  $T_1$ , for a time,  $t_H$ .
3. Cooling at a constant rate,  $m_3$  (often slower than the heating rate), until the reactions are quenched.

Under these conditions, the basic first-order rate equation for a single reaction,

$$\frac{dV_i}{dt} = k (V_i^* - V_i) e^{-\frac{E}{RT}}$$

may be integrated, subject to the approximation  $E/RT \approx 1$ , to yield

$$\frac{V_i^* - V_i}{V_i^*} = \exp \left\{ -k \left[ \frac{RT_1^2}{E} \left( \frac{1}{m_1} + \frac{1}{m_3} \right) + t_H \right] e^{-\frac{E}{RT}} \right\}$$

where  $V_i$  is now the total yield from the reaction.

For the distributed activation energy model, the corresponding equation is

$$\frac{V_i^* - V_i}{V_i^*} = \frac{1}{\sigma \sqrt{2\pi}} \int_0^{\infty} \exp \left\{ -k_0 \left[ \frac{RT_1^2}{E} \left( \frac{1}{m_1} + \frac{1}{m_3} \right) + t_H \right] e^{-\frac{E}{RT}} \right\} \cdot \exp \left\{ -\frac{(E-E_0)^2}{2\sigma^2} \right\} dE$$

This latter equation may be applied to the yield of any individual component, provided that the yield can be approximated by the assumed Gaussian distributions.

In the event that a more complex time-temperature history is followed (e.g., if  $m_1$  and  $m_3$  are not constants), then recourse may always be had to numerical methods for calculating the final integrated yield from the model.

REFERENCES

1. J. H. Campbell, "Pyrolysis of Subbituminous Coal in Relation to In Situ Coal Gasification," Fuel 57, 232 (1978).
2. E. M. Suuberg et al., "Product Composition and Kinetics of Lignite Pyrolysis," ACS National Meeting, New Orleans, March 1977.
3. W. B. Russell et al., "The Cities Service Model for Short Residence Time Hydro-pyrolysis of Coal," presented at 70th Annual AIChE Meeting, New York City, 14 November 1977.
4. D. B. Anthony and J. B. Howard, "Coal Devolatilization and Hydrogasification," AIChE Journal 22 (4), 625 (1976).
5. N. Gardner et al., "Catalyzed Hydrogasification of Coal Chars," Advances in Chemistry Series, No. 131, p. 217 (1974).
6. V. T. Ciuryla et al., "Ambient-Pressure Thermogravimetric Characterization of Four Different Coals and Their Chars," Fuel, to be published.

TABLE 1

ANALYSIS OF COALS

<u>ASTM Rank</u>	<u>State</u>	<u>Ultimate Analysis (% Dry)</u>					
		<u>C</u>	<u>H</u>	<u>N</u>	<u>S</u>	<u>Ash</u>	<u>O</u> (By Difference)
Lignite	ND	61.6	4.1	1.1	0.6	10.0	22.6
Lignite	TX	64.5	4.2	1.4	0.9	10.0	19.0
Subbituminous	WY	66.4	4.6	1.0	0.8	6.0	21.2
HVC Bituminous	IL	66.4	4.6	1.1	4.5	10.6	12.8
HVA Bituminous	PA	80.5	5.0	1.2	1.1	5.0	7.2

TABLE 2  
KINETIC PARAMETERS

Component	Parameter <sup>+</sup>	Coals				
		North Dakota Lignite	Texas Lignite	Wyodak	Illinois No. 6	Pittsburgh
H <sub>2</sub>	E <sub>0</sub> , kcal/mol	72.8	76.9	73.1	73.7	74.6
	σ, kcal/mol	8.8	9.8	8.0	8.6	8.2
	v*	0.010	0.009	0.009	0.010	0.011
CO (1st Peak)	E <sub>0</sub> , kcal/mol	51.9	52.2	50.8	--	--
	σ, kcal/mol	7.8	6.8	6.0	--	--
	v*	0.025	0.018	0.022	--	--
CO (2nd Peak)	E <sub>0</sub> , kcal/mol	70.3	72.7	71.2	66.7	71.1
	σ, kcal/mol	6.5	5.1	7.5	13.4	11.6
	v*	0.043	0.036	0.053	0.038	0.021
CO <sub>2</sub>	E <sub>0</sub> , kcal/mol	48.9	53.0	50.3	55.6	61.8
	σ, kcal/mol	9.5	11.4	9.6	14.2	18.1
	v*	0.134	0.123	0.100	0.040	0.015
CH <sub>4</sub>	E <sub>0</sub> , kcal/mol	57.7	60.1	58.2	58.8	58.7
	σ, kcal/mol	6.0	7.0	5.9	5.8	4.8
	v*	0.016	0.021	0.021	0.022	0.030
Total Weight Loss	E <sub>0</sub> , kcal/mol	52.7	52.5	53.2	53.0	51.8
	σ, kcal/mol	11.3	10.0	9.7	9.3	5.7
	v*	0.40	0.40	0.41	0.34	0.30

<sup>+</sup>k<sub>0</sub> is fixed at 10<sup>15</sup> min<sup>-1</sup> in all cases.

TABLE 3  
CAMPBELL'S PARAMETERS FOR WYODAK COAL

<u>Component</u>	<u>E<sub>0</sub>, kcal/mol</u>	<u>k<sub>0</sub>, min<sup>-1</sup></u>	<u>V<sup>*</sup>, g/g coal</u>
H <sub>2</sub>	22.3	1200	0.0102
CO, Reaction 1	18.0	3300	0.016
Reaction 2	30.1	1.5 x 10 <sup>5</sup>	0.037
CO <sub>2</sub> , Reaction 1	19.5	3.3 x 10 <sup>4</sup>	0.055
Reaction 2	23.0	1.4 x 10 <sup>4</sup>	0.047
CH <sub>4</sub> , Reaction 1	31.1	1.0 x 10 <sup>7</sup>	0.014
Reaction 2	31.1	1.7 x 10 <sup>6</sup>	0.016
Reaction 3	35.4	1.8 x 10 <sup>6</sup>	0.014

TABLE 4  
SUUBERG'S PARAMETERS FOR NORTH DAKOTA LIGNITE

<u>Component</u>	<u>E<sub>0</sub>, kcal/mol</u>	<u>k<sub>0</sub>, min<sup>-1</sup></u>	<u>V<sup>*</sup>, g/g coal</u>
H <sub>2</sub>	88.8	9.5 x 10 <sup>19</sup>	0.0050
CO, Reaction 1	44.4	1.1 x 10 <sup>14</sup>	0.0177
Reaction 2	59.5	1.6 x 10 <sup>14</sup>	0.0535
Reaction 3	58.4	3.5 x 10 <sup>11</sup>	0.0226
CO <sub>2</sub> , Reaction 1	36.2	1.3 x 10 <sup>13</sup>	0.0570
Reaction 2	64.3	3.5 x 10 <sup>15</sup>	0.0270
Reaction 3	42.0	3.3 x 10 <sup>8</sup>	0.0109
CH <sub>4</sub> , Reaction 1	51.6	9.7 x 10 <sup>15</sup>	0.0034
Reaction 2	69.4	2.8 x 10 <sup>16</sup>	0.0092

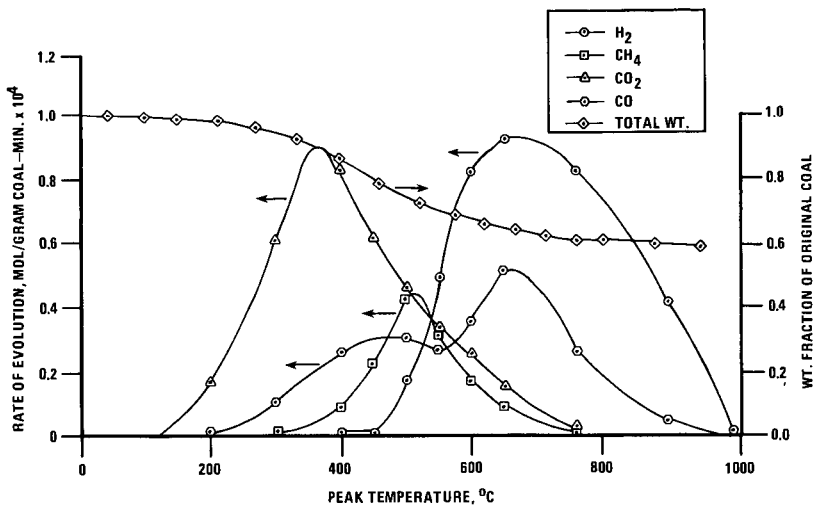


FIGURE 1.  
PYROLYSIS YIELDS FROM A NORTH DAKOTA LIGNITE

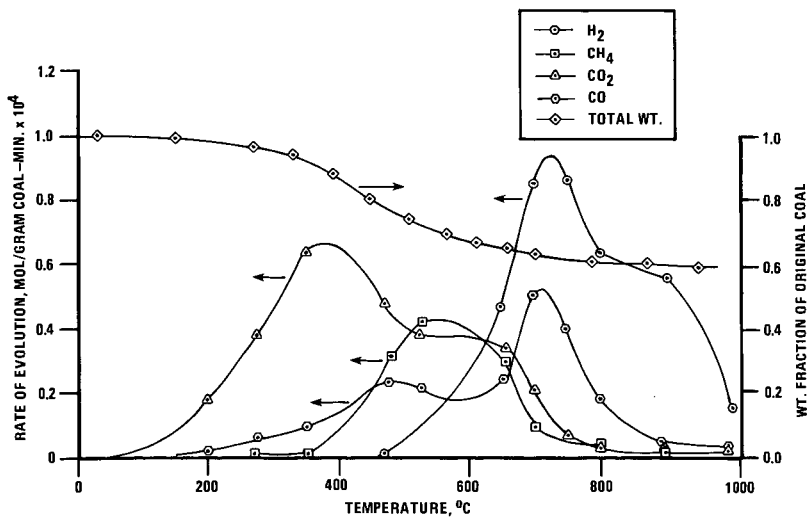


FIGURE 2.  
PYROLYSIS YIELDS FROM A TEXAS LIGNITE

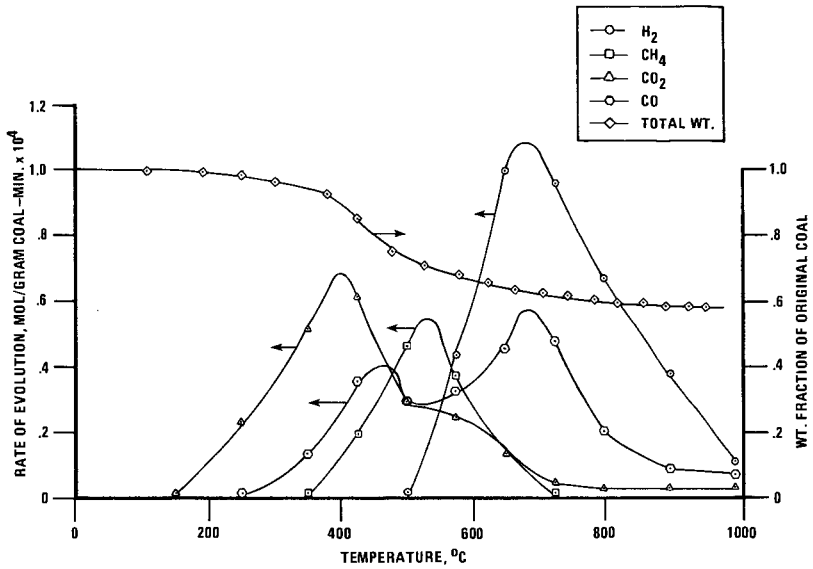


FIGURE 3.  
PYROLYSIS YIELDS FROM A WYODAK COAL

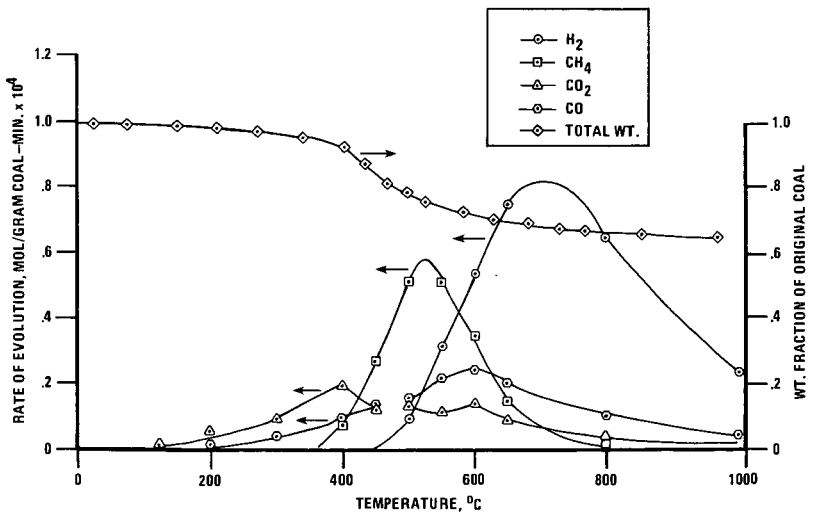


FIGURE 4.  
PYROLYSIS YIELDS FROM AN ILLINOIS NO. 6 COAL

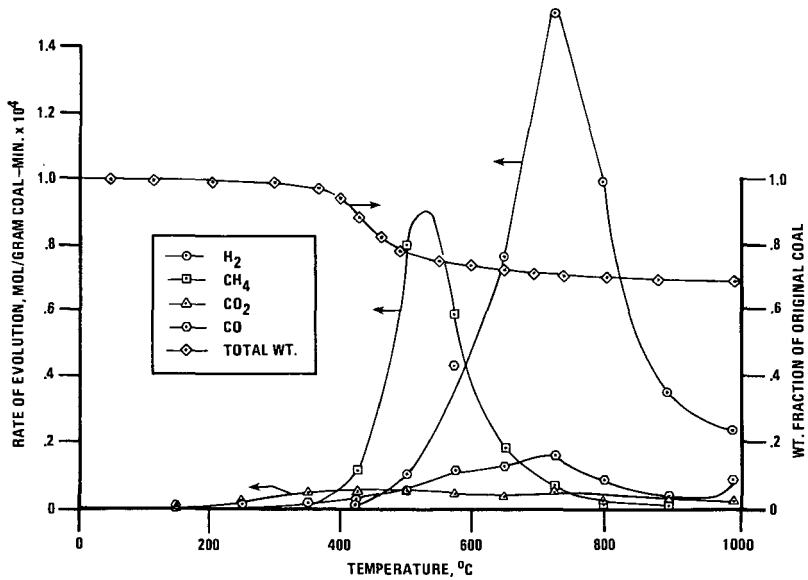


FIGURE 5.  
PYROLYSIS YIELDS FROM A PITTSBURGH SEAM COAL

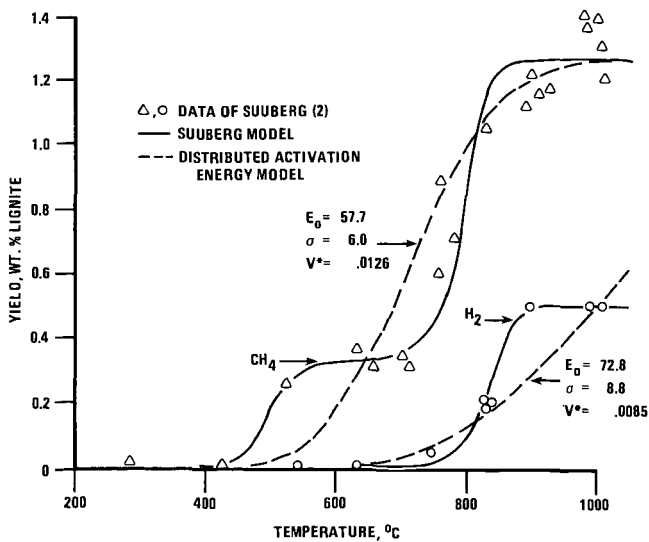


FIGURE 6.  
YIELDS OF METHANE AND HYDROGEN VIA FLASH  
PYROLYSIS OF MONTANA LIGNITE

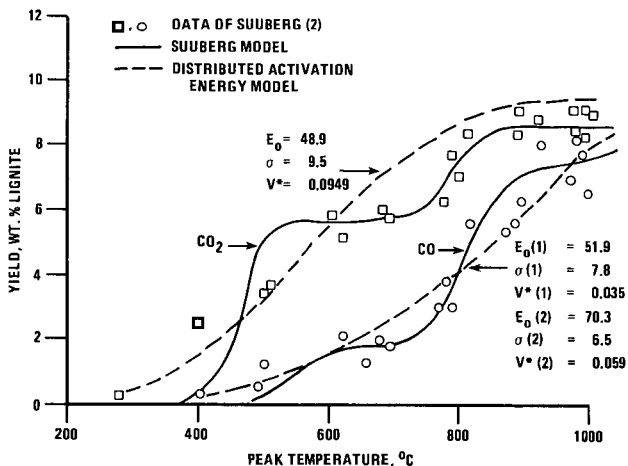


FIGURE 7.  
 YIELDS OF CO AND CO<sub>2</sub>  
 VIA FLASH PYROLYSIS OF MONTANA LIGNITE

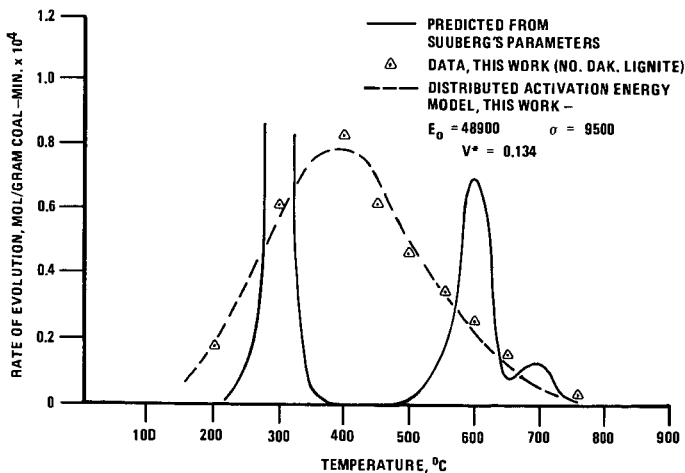


FIGURE 8.  
 CO<sub>2</sub> PRODUCTION RATE  
 VIA SLOW PYROLYSIS OF LIGNITES